ADDIS ABABA UNIVERSITY
SCHOOL OF GRADUATE STUDIES

Seismic Microzonation For Central Addis Ababa

By
Araya Mengistu

INSTRUCTORS' PROVISION OF WRITTEN RESPONSES TO STUDENTS' BUSINESS LETTER WRITING

By: Masresha Teferi

Approved by Board of Examiners

_____	_____
Advisor	Signature
_____	_____
Examiner	Signature
_____	_____
Examiner	Signature

ADDIS ABABA UNIVERSITY
SCHOOL OF GRADUATE STUDIES

Seismic Microzonation
For Central Addis Ababa

By Araya Mengistu

Approved by Board of Examiners

Dr. Messele Haile	_____
Advisor	Signature
Dr.-Ing. Samuel Taddese	_____
External Examiner	Signature
Dr.-Ing. Asrat Worku	_____
Internal Examiner	Signature
Dr.–Ing. Derege Hailu	_____
Chairperson	Signature

Seismic Microzonation
for
Central Addis Ababa

A Thesis submitted to
School of Graduate Studies
Addis Ababa University

In partial fulfillment of
The requirements for the
Degree of Masters in Civil Engineering

By Araya Mengistu
July, 2003

Acknowledgements

This study was conducted under the supervision of my advisor, Dr. Messele Haile of Civil engineering department, Addis Ababa University. I would like to express my deepest gratitude to him for his helpful guidance through out the research work and for providing me with relevant materials.

I would also like to extend my gratitude to Ato Yoseph Haile for his extensive help during measurement works.

Finally, I would like to thank W/t Axumawit Tadesse for her profound encouragement and enormous help through all the years of my study and this research work. Thanks also to Dr. Bewketu Tadesse, for helping me in printing and compiling works.

Table of Contents

List of Tables

List of Figures

Abstract

This study is conducted to prepare seismic microzonation map to central part of Addis Ababa City. The basic method used is the observation and analysis of microtremors.

The first effort was made by Ayele (2001) based on 40 observation sites. Latter detailed study was initiated by dividing the city in to five parts namely the northeastern, northwestern, central, southeastern and southwestern parts of which the central part is the study area for this thesis.

In this thesis seismicity and related hazard for Addis Ababa city and its locality, historic records, geologic conditions and effects on earthquake, and the theoretical background used in preparing microzonation maps are presented. The nature of microtremors, basic characteristics and their use in estimating site-effects is also discussed together with the method of measurement, equipments used and available tools to analyze collected data. The suitability of microtremor based site-effect study has been tested by comparison of results with solutions from one dimensional analytical model for selected sites.

Introduction

Earthquakes happen as natural disaster throughout the world. Their occurrence and potentially destructive damage on human lives and infrastructure, especially in developed and populated areas is a concern of increasing scale in modern world. Their effect on business and industrial zones including nuclear power stations and hazardous waste disposal areas is also an additional concern.

In Ethiopia, Earthquakes have occurred many times in the past. This can be confirmed from the literature and historical records [11]. This has initiated earlier studies on earthquakes and related hazard assessments. Currently hazard levels due to expected earthquake occurrences are available in the form of regional seismic zonation map of the country. Addis Ababa city is an important center for the country, and the continent. Numerous governmental, international and business organizations are found in the city, and the construction of municipal infrastructure is ever increasing. The city is located on the western ridge of the Great Rift Valley, which is among the tectonically active areas of the world. Due to this fact, recurrence of earthquake poses a significant risk in the area. The occurrence of earthquakes in Ethiopia in general and Addis Ababa city in particular can be established from historic and instrumental records over the years [1, 11].

The level of hazard due to earthquake occurrence of a certain magnitude / intensity can be significantly affected by surface geology, which can vary appreciably within close proximities. This fact necessitates the preparation of seismic microzonation maps that account for local site effect. These maps enable proper planning and implementation of municipal infrastructure and civil works with sufficient consideration of seismic hazards associated with the particular area of interest.

This work intends to produce a local hazard map for the central Addis Ababa, which can be vital for:

- Land use planning,
- Safe structural design, and
- Planning of mitigative measures for the probable earthquake occurrences.

Background

The goal of seismic microzonation of an urban area is to asses the dynamic response behavior of sites during a possible earthquake and grouping of areas with similar characteristics in to a category. This enables to improve structural design of buildings and infrastructure, and their performance during earthquake occurrences. Seismic risk at a particular area is defined as

*Risk= Hazard * Vulnerability*

Seismic hazard is a function of the probability of occurrence of earthquakes as natural phenomena. The potential destructive effect of earthquakes on superstructures and the environment is related to the degree of vulnerability. Endangered human lives constitute the greatest extent of damage in vulnerability assessment. Massive fault rupture, soil liquefaction, landslides and large-scale settlement of loose soil deposits are major environmental impacts. Depending on the amplification characteristics of the site soils involved, the damage to various infrastructures is also of great concern.

Various methods and techniques could be used to prepare a seismic microzonation map for an area, which include:

- The study of damage patterns on structures due to past earthquakes,
- Study of strong ground motion records and associated response of soil deposits,
- Analytical or theoretical methods, which use geophysical and geotechnical data of the site, and
- Microtremor observations.

The reliability of the results of a seismic microzonation effort depends on the quality of available data, and the method used. The use of a combination of the above approaches is always encouraged in order to come to better results. In the context of Addis Ababa city, the first two methods are not applicable, as records for earthquakes and associated damage pattern are not available. Information from geophysical / geotechnical methods has been used in a limited way to estimate site response with the aid of numerical simulation tools. Another method gaining significant popularity among researchers worldwide is the use of microtremor observation. The recorded microtremors can usually reflect site-effects with good agreement to results from simulation models or actual ground motion records. The advantages of the method include:

- Minimum manpower requirement for data collection and analysis
- Ease of operation
- Small cost of exploration and instrumentation
- Required data acquired very quickly, saving time
- Minimal disturbance to surrounding

In this study, microtremor observation is used for the purpose of seismic microzonation. It is part of an effort to produce a microzonation map to the whole city. The first work was done by Ayele (2001), which was based on 40 observation spots throughout the city

(see Fig. 1-1). As a pilot research, it included methods and means to assess the applicability of microtremor based site effect study particularly to Addis Ababa. The work has indicated that the method can be applied [4]. Latter a detailed study of the city by subdividing it into North-eastern, North-western, western, Central, South-western and South-eastern regions was launched. The portion of the study for the Southeastern part was completed recently, by Abera (2001) [2]. This study was conducted based on microtremor observation at 90 sites. (See Fig. 1-2)

The method of analyzing microtremor records to characterize site-effects used in this thesis has been used in different parts of the world, and has shown good potential in predicting surface motions induced by earthquakes. The applicability of the method particularly to Addis Ababa is tested in the two previously mentioned works, and generally acceptable results are documented. In this research, comparison with analytical solutions is also included to strengthen these findings, and further consolidate the issue of applicability.

Objective

The seismicity of Addis Ababa city can be considered moderate. The current practice of 'disaster resistant' structural design accounts for a certain level of acceleration due to an earthquake of certain recurrence, which is constant for a given region – as in the seismic zonation map for Ethiopia.

The effect of surface geology and soil formations on both the frequency content and amplitudes of vibration is accounted for in an insufficient manner. However this effect is very significant. Design practices should incorporate these local effects if truly 'disaster resistant' civil structures are to be realized. Also, the process of planning realistic mitigative measures during possible disastrous earthquake occurrences requires the knowledge of localized effects. The evaluation of seismic hazard in municipal areas and other vulnerable localities should include the study of local site-effects as a major input.

The city of Addis Ababa is being studied for site-effects with the final goal of producing a seismic microzonation map. As part of this effort, this research aims at studying the central part of the city, which compliment the other studies to provide a complete seismic microzonation map of the city. The objective of the study is to produce a microzonation map for the study area, by using the following parameters:

- Predominant period
- Fourier amplitude

Figure 0-1: Microtremor measurement points as used by Ayele. [4]

Figure 0-2: Microtremor observation spots used for the study of Southeastern Addis Ababa. [2]

Methodology

Various ways of attaining a seismic microzonation map exist. They are practiced in parts of the world based on their suitability, adaptability and local experience. For this study, the method of microtremor measurement is used. Three high-sensitivity seismometers are used to record microtremors at various spots. The data are recorded on a computer, with seismometers connected to it as peripheral devices.

The analysis of the data is made using conventional Fourier Transformation for spectral analysis. Site characterization is made by studying variation of the spectral plot for different segments of the recorded time history, both in frequency content and in amplitude.

The results from the Fourier analysis are further processed using Arch view software for depicting the spatial variation of parameters, and also for microzonation of areas of similar characteristics.

The following limitations are encountered in the various stages of the development of this work:

(1) Few borehole data with little information on soil index properties are available for analytical modeling. A good correlation has been observed. However, more data with better quality should be used in future works.

(2) The use of geotechnical databases in analytical solution to determine response behavior mainly involves use of empirical relations, which correlate a test parameter with (a set of) dynamic properties. In this thesis, Plasticity Index (PI), unit weight, and blow count records from SPT have been widely used. As laboratory/field test results usually depend on numerous factors, a method to account for uncertainty levels of acquired data may be a good supplement in deciding the degree of reliability.

(3) N values for SPT tests are known to vary appreciably even at near by sites. Test procedures and equipment type significantly affect blow count records, despite standardization efforts worldwide. In this thesis, the effort to examine acceptable levels of Energy Transfer ratio (ETR) for use in estimating equivalent blow count (N_{60}) values has succeeded fairly.

(4) In general, geotechnical explorations are essential for many researches and design/analysis works. Their availability in sufficient quantity and quality is of crucial importance to the success of similar works. Enterprises/Organizations in exploration tasks should be committed to building a quality database and provide support to such endeavors.

Surface Geology and Seismicity of Central Addis Ababa

The Study Area

Addis Ababa city is an important center for the country economically and politically. It is located on 09^0 02' N (Latitude) and 38^0 43' E (Longitude). The city occupies a total area of about 360 square kilometers [27]. The central part of the city, which is addressed in this study, approximately constitutes about 14 square kilometers.

The delineated area encompasses established centers of commerce such as Merkato, Teklehaimanot and Arada areas; places of political significance such as the Congress Hall, Presidency Palace, ECA, UNDP, UNESCO, and UNICEF buildings; Symbols of architectural excellence such as the City Council of Addis Ababa, and the Main Branch of Commercial Bank of Ethiopia; major health facilities of the city as the Tikur Anbessa, Menilik and Yekatit 12 hospitals; top class hotels and resorts of choice such as the Sheraton Addis and the Hilton Hotel; prominent educational facilities such as the AAU and its various campuses; emerging high riser buildings like Nani building, and Arada Complex. Figure 2-1 and 2-2 show the study areas for overlaying the woreda map of the city and the delineated area of interest for this study, respectively.

Figure 0-1: Woreda Map of Addis Ababa city, showing study areas for central and southeastern parts.

Figure 0-2: Delineated area for Central Addis Ababa, showing woredas and the road network.

Local Geology

The geological and engineering geological information on the city of Addis Ababa is compiled in [26]. The city of Addis Ababa is generally covered by volcanic rocks, with northern part of the city predominantly covered with rhyolite and trachytic rocks.

Southern part of the city, such as Wochecha (SW), Furi (S) and Yerer (SE) are mainly trachite in composition. In some parts of the central part and scarcely in Entoto hills, basalts outcrop. Rock outcrops identified from the engineering geological map of the area

under study are of very high to medium strength. Most faults observed in the city are of NE-SW orientation, which is the same as the main Ethiopian rift fault. The dominant fault in the central part of the city is the Filwoha fault. [26]

Kebena and Ketchene rivers are main drainages in the delineated area, which at parts of the city (i.e., in low elevation areas further in the southern vicinity) are observed to form terraces of alluvial deposits. The central part, as can be seen from figure 2-3, is dominated by residual soils. These soils exhibit intermediate to high plasticity.

Seismic occurrences experienced in the past have been compiled in P. Guin (1978) [11]. The region has almost continuously been jolted by tremors – as evidenced from historic and instrumental records spanning over six centuries. The horn in general experiences movement from the rift valley system and the red sea. Addis Ababa city in particular has experienced shocks of varying magnitude not only from far epicenter sources – but also from with in the vicinity of the city itself.

Figure 0-3: Local geology in Central Addis Ababa, showing soil cover variation. [26]

Figure 0-4: Map of Major tectonic features in Ethiopia [11]

The existence of seismic activities aroused the awareness of [Ethiopian] authorities, so that early studies on localization, recurrence and amplitude hazards to life due to earthquake occurrence were initiated. This effort has been progressively updated with increased data from instrumental records and recent perspectives of seismology. Currently, based on the updated data, a seismic zonation map is available for the country.

Seismicity of Addis Ababa

Seismicity is defined as 'the frequency per unit area of earth quakes in a given region'. However, the term is often used to denote ' seismic activity of a given region -an indication of seismic energy released' - and is more meaning full to engineering purposes in this sense [7].

Figure 2-5 depict epicenter locations for past earthquakes felt / recorded till 1975 in Ethiopia. From the epicenter location maps it is obvious that epicenters in Ethiopia are almost exclusively related to the outline of the Great Rift Valley. The city of Addis Ababa is located on the western ridge of this valley. As a result, earthquake experience of

the city has been observed on many occasions. The 1906 and 1961 earthquakes are few of most felt cases, which resulted in extensive panic of the residents of the city [1].

The seismic hazard map for Ethiopia is presented in EBCS 8 as shown in figure 2-6, which subdivides the country in to seismic zones depending on the local hazard. The hazard within each zone, by definition, is assumed uniform. The seismic zonation map of the country shows the distribution of the expected hazard, which follows the physical boundaries of the Rift Valley itself. Areas, which are near the valley, experience more hazard than those located far away.

However, the map is a regional hazard map, and hence has limitations in representing site-specific responses for different parts of the city. The significant influence of response of soil deposits on structural behavior necessitates the incorporation of this vital information in the development of seismic microzonation maps.

Figure 0-5: Epicenter location of earthquakes till 1975 with magnitudes equal to or greater than 5 in Ethiopia. [11]

Effects of Surface Geology on Seismic Motion

The term topographic condition is used to describe both the material and geomorphologic conditions of a site. The latter tend to alter or modify the amplitude, frequency content and duration of the ground motion - thus being of particular importance especially in seismic design of structures [9]. Because of the enormous

Figure 0-6: Seismic Zonation map of Ethiopia [18]

variations expected from site to site, geomorphologic features cannot be incorporated in to building /structural design codes, demanding site-specific studies.

Local site effects on ground motion include effects on the frequency content and the amplitude of motion. Usually there is a shift of predominant period to a value corresponding to the period of resonance of the soil deposit. The maximum Fourier amplitude of the spectral plot – corresponding to the amplification characteristic of the soil under study – is obtained at resonant frequency. Hence, a more or less similar dynamic response behavior may be expected at a given site for even different earthquakes. This shows that local geologic conditions need sufficient consideration in the study of earthquakes and their potential effect.

A case study, as presented by Yegian et al (1944), is the damage pattern investigation in Kirovakan during the 1988 Armenia Earthquake [24]. It was shown that 98% of the collapsed buildings were located with in a few blocks, whose soil profile consisted an alluvial valley of stiff clay.

Investigation of site-effects is made by the study of characteristics of transfer functions, which are ratios of the motions observed at the surface to that at the rock bed. Empirical transfer functions of a site can be obtained from the ratio of Fourier transforms of seismogram observations at sediment sites and that at a nearby rock site - usually referred to as "Strong Motion Spectral Ratio" or SMSR method. It has been a well-established procedure to try to estimate site-specific response characteristics to earthquake excitation from either "Theoretical Transfer Function" (TTF) or "Horizontal to Vertical Spectral Ratio" (HVSR) of micro-tremor observations. Various researchers have shown that a strong correlation holds between estimates of site response characteristic from the three methods.

The determination of effects of site amplification characteristics on strong ground motion requires availability of seismic record data at suitable sites, i.e., observation site and rock bed site. These data are very expensive to obtain requiring a network of seismogram instrumentation, and are not always available. Hence, it is customary to adopt analytical procedure, as not only alternative methods of strong ground motion study but also as stand alone simulation tools, to supplement site effect studies.

While both types of records, i.e., strong and weak motion records can be used for seismic microzonation; strong ground motion data gives more representative results of ground response to an earthquake occurrence than weak motion records. In the context of Addis Ababa city, the former method has a limitation of recorded data availability. On the other hand, the use of weak motion records, such as microtremors, may fail to predict actual ground excitation levels, because of the strain levels involved. Hence, the use of the method to the purpose of site effect study should incorporate clear understanding of the nature and properties, before application.

Microtremors: Characteristics, Observation and Interpretation

Introduction

Fundamental characteristics of microtremors and the conditions of application to earthquake engineering have been discussed since the 1985 Mexico earthquake. In this earthquake, for example, the characteristics of microtremors seemed very clear and comparable with strong ground motion record at the same place. [16]

Microtremors are vibrations sensed at some point on the ground surface resulting from waves of various natures. The vibration is a result of change in stress state due to some input disturbance. The vibration readily passes through the different geological units (rocks and soil deposits). Some waves are found only at/or near the surface (surface waves) and others pass through the volume of a material (body waves). Body waves are the fastest of all seismic waves.

Surface waves, on the other hand, travel only near the boundary, and attenuate rapidly with distance from the surface. They can be further classified as Love and Rayleigh waves. Surface impacts, explosions and waveform changes at boundaries produce surface waves. They can also be portions of surface wave trains in earthquakes.

Nature and characteristics of Microtremors

Ground motions emanating from some source travel through the soil deposit and are sensed at the location of measurement. The recorded microtremors may be a result of human or natural activity. Those due to the former have been studied and characterized by Kanai et al (1961), and are usually successfully identified from continuous measurements. They are characterized by daily variation of amplitude, getting larger in daytime and smaller in night-time; and existence of very stable predominant period as well. They are expected in alluvial and sedimentary deposits.

On the contrary, those vibrations occurring due to natural activities like sea waves and after shocks are known as microseisms. Their precise identification requires extensive knowledge of the governing activities, obtaining a clear and understandable trend is usually difficult. Rich database including worst season conditions should exist to reveal their presence and incorporate the effect on the study of site effects to seismic excitation.

Microtremors observed at the ground surface are not always steady, but usually shows daily, weekly and seasonal changes. This is because the tremor is affected by surrounding noise sources such as moving vehicles and running machines. As a result, frequency components of horizontal and vertical components of microtremors indicate effects of, not only local site conditions, but also such noise sources. A quick microtremor

measurement carried out in Mexico basin [16], and analysis of the observation confirmed the following:

- Very large variation of measured microtremors both in amplitude and in predominant period across the basin was confirmed showing the variation from time to time and place to place.

- Comparison of measured microtremors with strong ground motions records revealed an interesting point. A good fitting between the two was obtained only on soft sediments, but never on firm ground or lava flow showing microtremors dominate in soft sediment deposits.

- By using continuous measurements of microtremors at firm ground sites, it was found that principal component of the measured tremor was mainly composed of microseisms, and it did not reflect the site effects of the ground.

These observations render the use of microtremor based site effect study to be precautious, though obtaining the data is very simple, fast and very economical as compared to other techniques. The latter usually require identification of subsurface soil structure for an entire region and /or a network of seismograms over the area of interest.

Data, Analysis and Interpretation

Microtremors are measured on the surface of the ground by sensitive instruments (seismometers). The measurement equipment comprises three highly sensitive seismometers, to sense ground movement, and a special laptop computer to record the movement. An amplifier and A/D converter unit links the seismometers to the computer. During measurement, the seismometers are placed keeping standard North-South, East-West and Up-Down orientation using a compass. Figure 3-1 shows typical arrangement of the equipment during field measurement procedures. The equipment used in the measurement of microtremors for the purpose of this thesis includes a set of seismometers with a capacity to record the three orthogonal components.

Each data at a point has a velocity - time history record from three seismograms, each 300 seconds long and sensing vibration in the East-West (EW), North-South (NS) and Up-Down (UD) directions. Figure 3-2 shows a segment of one such record.

The use of measured microtremors for the study of site effects is based on the principle that, microtremors propagate in the ground and they are amplified at periods that are synchronous with the predominant period of the site due to features of selective resonance [14].

Figure 0-1: Basic setup of equipment during field measurement.

Mostly microtremor data are interpreted making use of Fourier analysis and computing spectral ratios taken at different sites by normalizing over a reference point. As an alternative method, a spectral ratio between the horizontal and vertical components is also used as an indicator of the site transfer functions. The use of horizontal to vertical spectral ratios method has been in use, since Nakamura first introduces it in 1989. The spectral ratio technique is a useful way to estimate empirical transfer functions to evaluate site effects. Standard spectral ratios are computed by dividing Fourier spectrum of ground motions observed at the surface, HS_s , to that of near by rock site, HS_b (or a reference station), as

$$RE = \frac{HS_s}{HS_B} \qquad \textbf{0-1}$$

Figure 0-2: Segment of typical time history plot for the three channels of measured microtremors.

Lermo and Chevas(1993) used spectral ratio A_s to estimate amplitude effect of source as:

$$A_s = \frac{VS_S}{VS_B} \qquad \textbf{0-2}$$

where VS_S and VS_B are Fourier spectra of vertical motions at the surface and bedrock at certain depth. Surface waves, particularly, Rayleigh waves impart some influence on vibration of soil particles on the surface, and the parameter A_s has been used to estimate the effect. If this effect is assumed to be the same on both the vertical and horizontal component vibrations, then A_s can be used to eliminate the effect. A modified site transfer function, R_M, can then be introduced as

$$R_M = \frac{R_E}{A_S} = \left(\frac{HS_S}{HS_B}\right) * \left(\frac{VS_B}{VS_S}\right) \qquad \textbf{0-3}$$

It has been observed (Nakamura, 1989; Huang and Chung, 1977) that the ratio (HS_B/VS_B) is nearly 1.0 for micro-tremor observations in boreholes and earthquake records as well. [15]

With these empirical checks, the transfer function can be reasonably estimated as:

$$R_M = \frac{HS_S}{VS_S}. \qquad \textbf{0-4}$$

Lermo and Chevas (1993) applied the method to estimate empirical transfer functions for the intense part of small samples of earth quake records obtained in three cities in Mexico, and their results show that *H/V* ratio can give robust estimate of frequency and amplitude of the first resonant mode, but not for higher modes.

Field et al (1995) considered the response of sedimentary layers to ambient seismic noise and suggest that *H/V* ratio is an effective and reliable tool to identify the predominant period estimated from the thickness of an alluvial layer. Other similar studies showed that the *H/V* spectral ratio depicts well the fundamental resonant frequency. The *H/V* spectral ratio method has been used in subsequent analysis and characterization of measured microtremor data for site-effect study in this thesis.

Site Effect Study from Microtremors

Microtremor observation and analysis has served as an alternative method of site-effect studies in many projects. A number of studies show existence of good correlation between weak and strong motion site response. These studies demonstrated that under certain circumstances and with certain limitations, microtremors could be used to estimate strong motion response. In particular, it is possible to identify the fundamental period of surface layers that have a sharp impedance contrast to their substratum.

In a research carried out in Yokohama city of Japan [25], a record of 150 accelero-grams distributed all over the city were analyzed and compared with results from micro-tremor observations. It was found out that:

- For most sites, the fundamental periods of strong motion spectral ratio and analytical methods are, almost, of the same value as that obtained from micro-tremor data analysis.
- Spectral amplitudes of the Strong motion spectral ratio (SMSR) and Theoretical transfer functions (TTF) increase with those of *H/V* of microtremors, and the following trend is observed:

$$A_{SMSR} = 0.83\ A_{H/V}$$

Showing amplitude estimate from the latter methods is usually larger than actual (observed) values, and

- Correlation between spectral characteristics of SMSR and those of H/V is higher than between TTF and H/V, mainly because assumed soil structure may not correctly / sufficiently represent the actual conditions.

It can be observed that, actual ground response is not very much different from that obtained by either theoretical transfer functions or by analysis of microtremors. Consistent trend can be observed in various works, which guarantee the use of simple and cost effective methods as microtremor observation, whenever data is not available to adopt the other methods. The following limitations should be observed before applying microtremor observation to characterize strong or moderate ground motions. [13]

- Microtremors operate at very low strain levels when compared to strong ground motions, which result in higher strain levels inducing non-linearity.
- The effect of source on microtremors is significant. Removing the effect of these sources is not so direct.
- Microtremors are more difficult to apply when subsurface formation is complicated.

Non linear effects have the tendency to reduce the amplitudes of spectral peaks and shift them towards longer periods. The existence of clear contrast in dynamic soil properties between layers determines whether the method can work well in predicting site effects. A comparison of measured microtremors between damaged and non-damaged areas after the occurrence of an earthquake in different areas in Northridge, [16] shows this fact. As can be seen from figure 3-3, microtremors in damaged areas and in non-damaged areas do not show noticeable difference at all sites

Figure 0-3: Comparison of microtremors in damaged & non-damaged areas.

Generally, one can expect microtremors to explain the characteristics of observed seismic motions with in certain limitations. It can also be noted that, comparison of such results with geotechnical data and seismic motion records are expected, if the outcomes are to be considered representative of the site effects. In this research comparison of results with analytical solutions derived from geotechnical data is made at selected sites, before applying the method in the study area.

Applicability Studies

Introduction

Generally, all methods used to estimate response of soil deposits to earthquake excitation involve a certain degree of uncertainty due to input data quality and assumptions related to the formulation of the methods themselves. The choice of a specific method for application in a certain area is determined by availability of data and adaptability of the method to the area. In order to increase the reliability of the results, adequate evaluation of the methods for possible application should be carried out. In light of this, this chapter aims at evaluating the applicability of microtremor based site effect study to Addis Ababa, by using analytical methods.

Therefore, the approach exercised here is to select model sites and determine response parameters using analytical methods. Latter microtremor observations are carried out at the identified sites, and analysis is carried out to obtain values of the required parameters. A comparison between results from the two methods will then give indications on the applicability of microtremor based site-effect studies. If results obtained from microtremor analysis is comparable to that obtained from the analytical method, then the method of microtremor observation and analysis for application in site effect studies can be justified. If not, the method may require further investigation on its applicability for the study area before use.

Analytical Methods

In many engineering practices analytical models are developed and used to simulate natural phenomena. In the study of earthquake motion and related hazard assessment, various models have been in use, which include 1D, 2D and 3D models. The level of sophistication and input data requirement (in terms of both quantity and quality) increases for higher dimensions.

The obvious choice of 3D analysis to simulate source and path effects of natural basin as it occurs is confronted with the limitation of extensive database requirement on soil and rock properties, which are not always available. The assumptions made to fill the gaps in the database are usually sufficient to deem the 3D solution futile. In fact, the data usually found is so limited that use of 3D models is not considered as a reliable tool. Major limitations include:

- Bedrock topography
- Soil stratigraphy, and
- Dynamic properties accounting for material non-homogeneity for each of the identified soil layer.

Furthermore, computational limitations also pose considerable complication. Examples are applicability and efficiency of numerical solution schemes (FD, FEM), computer memory and time requirement.

The 2D analysis is usually considered to be a reasonable tool to utilize, if the site conditions justify the use. A small variation in general soil stratification and property in one of the two (horizontal) orthogonal directions may justify further consideration of 2D analytical methods for use in simulating ground excitation.

On the other hand, 1D analysis require usually available data from geotechnical / geophysical explorations and are computationally easy. However serious limitations of accounting for effects of irregularity in soil strata and bedrock orientation exists. In this thesis, the 1D analysis has been adopted, as the existing database is not encouraging to consider the other two.

1D analysis

One-dimensional analysis is made by multiple reflection theory of vertically propagating horizontal components of shear waves through multi layered soil profile. A complete documentation on the methods and applications of this analysis is found in various texts, and also in [18].

The basic equation of motion is given by

$$\rho(z)\frac{\partial^2 u(z,t)}{\partial t^2} = \frac{\partial \tau(z,t)}{\partial z} \qquad \textbf{0-1}$$

where

$\rho\,(z)$ is density of the soil material,
$u\,(z)$ is the displacement perpendicular to the vetical axis, and
$\tau(z)$ is shear stress defined by

$$\tau(z) = G\gamma + \eta\frac{\partial \gamma}{\partial t} \qquad \textbf{0-2}$$

Where

G is shear Modulus,
γ is the shear strain, and
η is the viscosity.

Depending on the conditions of the soil property accounted for in the analysis, the shear stress τ may exhibit linear or non-linear behavior. Substituting equation 4-2 in equatoin (4-1) and using the relation,

$$\gamma = \frac{\partial u}{\partial z} \qquad \textbf{0-3}$$

the governing equation of motion will be

$$\rho(z).\frac{\partial^2 u(z,t)}{\partial t^2} = G\frac{\partial^2 u(z,t)}{\partial z^2} + \eta\frac{\partial^3 u}{\partial z^2 \partial t} \qquad \textbf{0-4}$$

The solution of the above equation to linear and Equivalent Linear methods of analysis is outlined below.

Linear Analysis

Considering the layered soil system such as that in figure 4-1, the vertical propagation of shear waves induces displacements in every layer. The frequency response function between any two layers for a linear solution is given by [21]

Figure 0-1: Layered soil system.

$$H_{m/n}(\omega) = \frac{A_m + B_m}{A_n + B_n} \qquad \textbf{0-5}$$

The amplification ratio can also be obtained from

$$A_{m/n} = \left|H_{m/n}\right| \qquad \textbf{0-6}$$

where

$$A_{i+1} = \frac{1}{2}\left[(1+R_i)A_i e^{iP_iH_i} + (1-R_i)B_i e^{-iP_iH_i}\right] \qquad \textbf{0-7}$$

$$B_{i+1} = \frac{1}{2}\left[(1-R_i)A_i e^{iP_iH_i} + (1+R_i)B_i e^{-iP_iH_i}\right] \qquad \textbf{0-8}$$

$$R_i = \frac{G^*{}_i P_i}{G^*{}_{i+1} P_{i+1}}$$

or

$$R_i = \sqrt{\frac{\rho_i G^*{}_i}{\rho_{i+1} G^*{}_{i+1}}} \qquad \textbf{0-9}$$

$$G^* = G_i(1 + 2i\beta_i) \qquad \textbf{0-10}$$

$$P_i = \omega\sqrt{\frac{\rho_i}{G^*{}_i}} \qquad \textbf{0-11}$$

in which R_i = impedance ratio, G^* = complex shear modulus, P_i = Propagation constant or wave number defined for specific layers. A MATLAB® code for obtaining linear solutions to soil models is attached in appendix F.

Equivalent Linear Analysis

The procedure described above utilizes the concept of linear analysis, where no account of the actual phenomena of soil non-linearity is made. Non-linearity of soil response behavior in stress - strain relations can be taken care of by the so-called equivalent linear analysis method. In this method an iterative procedure that considers the degradation in shear modulus and the increase in damping is utilized.

The input data being the shear modulus and damping ratio corresponding to small strain levels, i.e., G_{max} and γ, modified values for strain levels induced are obtained by iterative procedures. A new value of strain-time history is obtained for each set of Go and γ used, of which the effective strain equal to 0.65γ is used to obtain the next set of G and γ values. The process is iterated until a [preset] maximum percent error in computed values is achieved; or, alternatively, until a maximum number of iterations are completed.

Non Linear Models

Soil is supposed to behave in a non-linear manner when subject to ground motions involving higher strains / deformations - which is the case for earthquake magnitudes of moderate to high intensity. The evidence of non-linear soil behavior comes from experimental cyclic tests on soil samples, where departure from the linear response state is observed for large strains. In almost all cases of practical interest, the response under cyclic loading is best described to suit the requirement of sound analytical investigation only by considering the true nonlinear soil behavior.
Practitioners in the area of earthquake studies generally perform linear modeling of ground response even at strong ground motion levels. One reason is the linear behavior is shown to be effective to model strong ground motions. Another is that, amplification factors derived from weak- and strong-ground motion records gave more or less similar results [20]. For the analysis carried out in this thesis, non-linear models are not considered.

Soil Models: Dynamic and Static Properties of soil layers

As an input to the major part of the thesis, i.e., the applicability of microtremor based site effect study, use of geotechnical databases at various sites would be required to come to acceptable conclusions. However, obtaining data was not easy and the study in this chapter had to be limited to three sites. These are Site-I (Faculty of Technology); Site-II (Faculty of science) and Site-III (Mexico Area). The sites have been modeled for analytical solutions to compare analytical results with that from micro-tremor observation. The physical description of the sites as obtained from borehole logs is attached in appendix B.

Before dynamic analysis is carried out the original borehole data is processed for simplification of soil profile, and correction of recorded blow counts. The former is usually necessary because borehole logs are usually complicated. A procedure to this purpose has been documented in [21] and has been used in this thesis. Depending on the desired degree of simplification, a '*soil simplification coefficient*' (COEF) is varied in the range of 0.25-2.5. A higher value for COEF gives less number of layers in the resulting simplified soil profile. The basic operation comprises grouping of strata of similar grain composition and blow count (N) properties into one profile. The simplified soil profiles for the four model sites are shown below in figures 4-2 to 4-4.

Figure 0-2: Simplified soil profile for Site I

Figure 0-3: Simplified Soil profile for Site II.

Figure 0-4: Simplified soil profiles for Site III.

The relevant dynamic and static properties can be obtained form the various empirical and theoretical relations. Shear modulus of soils is an important parameter in simulation of dynamic response to earthquake excitation. However, the available data for the identified model sites do not include the data for this parameter, and empirical relations are used. G_0 (or alternatively denoted as G_{max}) can be estimated from one of the many empirical relations proposed by various researchers. The following are commonly used.

(i) $\boldsymbol{G_o} = 1200\ \mathbf{N_{60}}^{0.8}$ (t/m^2) Ohsaki & Iwasaki, 1973 (Ref 2) ***0-12***

(ii) $\boldsymbol{G_o} = 325\ \mathbf{N_{60}}^{0.68}$ (kips/ft^2) or

$= 1587.9\ \mathbf{N_{60}}^{0.68}$(t/m^2) Imai & Tonochi, 1982 (Ref 1) ***0-13***

(iii) $\boldsymbol{G_o} = 20{,}000\ \mathbf{N_{60}}^{0.333}\ \sigma_m^{\ 0.5}$ (lb/ff^2) or

$=1398\ \mathbf{N_{60}}^{0.33}\ \sigma_m^{\ 0.55}$ (t/m^2) Ohta & Gotto(1976) Seed (1986) ***0-14***

(iv) $\boldsymbol{G_0} = \rho \boldsymbol{V_s}^2$ (t/m^2). ***0-15***

In the above relations, N_{60} values represent effective blow count as corrected for overburden pressure, and energy transfer ratio (ETR). (See appendix-C.)

It can be seen that two variables influence computed values of period (T_0,) whose effect is not quantitatively known. Further more the variety of relations available for estimating G_0 values add to the level of uncertainty involved in the final results. The selection of a particular method for calculating G_0 values, and sensitivity analysis of object function period (T_0,) to the parameters COEF and ETR is made (see appendix C and E,

respectively). In further works, to calculate G_0, the relation by Ohta and Gotto (1976) (equation 4-14) is used.

To include the equivalent linear analysis, the trend in degradation of shear modulus and variation of damping with induced strain levels from the excitation need be determined. This is carried out for simplified soil profiles. Various researchers have proposed relations for G/G_{max} and critical damping ratio ξ. In this thesis, the following relation as proposed by Ishibashi and Zhang (1993) [15] is utilized.

$$\frac{G}{G_{\max}} = k\,(\gamma, PI)\;\sigma_m^{\,m(\gamma,PI)-mo} \qquad \textbf{0-16}$$

Where

$$K(\gamma, PI) = 0.5\left\{1+\tanh\left[\ln\left(\frac{0.000102+n(PI)}{\gamma}\right)^{0.492}\right]\right\} \qquad \textbf{0-17}$$

$$m(\gamma, PI) - m_o = 0.272\left\{1-\tanh\left[\ln\left(\frac{0.000556}{\gamma}\right)^{0.40}\right]\right\}e^{-0.0145\,PI^{1.3}} \qquad \textbf{0-18}$$

$$n(PI) = \begin{cases} 0.0.....PI = 0.0 \\ 3.37E-06PI^{1.4040}.....0 < PI \le 15 \\ 7.00E-07PI^{1.976}.....15 < PI \le 70 \\ 2.70E-09PI^{1.115}.....PI > 70 \end{cases} \qquad \textbf{0-19}$$

And, γ = strain (%), PI = Plasticity Index (%), σ_m = Mean effective confining pressure (KN/m^2)

Similarly, for damping ξ, Ishibashi and Zhang (1993) developed the following empirical relation for both plastic and non-plastic soils [15].

$$\xi = 0.333\,\frac{1+\exp(-0.0145PI^{1.3})}{2}^{2}\left[0.586\left(\frac{G}{G\max}\right)^2 - 1.547\frac{G}{G\max}+1\right] \qquad \textbf{0-20}$$

There are some laboratory tests for the unit weight and plasticity index of the soils under discussion. The latter, especially, is available for deposits containing appreciable amount of clay soils (See soil data in appendix C.) The variation of G/G_{max} and ξ versus strain (γ) thus obtained is shown in figures 4-5 to 4-7.

Figure 0-5: Plot G/G_{max} & ξ as a function of strain (γ) for Site I.

Figure 0-6: Plot G/G_{max} & ξ as a function of strain (γ) for Site II.

Figure 0-7: Plot G/G_{max} & ξ as a function of strain (γ) for Site III.

Analysis, Results and Discussions

In the previous section, the dynamic properties of the soils that make up subsurface profiles have been determined. The next step is simulation of the response behavior of the modeled sites. Different methods exist that can be used to run simulation of soil models, varying from one another in the input data, the method of analysis, and the output type. For the 1D analysis adopted in this study, the following methods have been used as applied for layered systems.

(i) $$T_0 = \frac{4H}{\overline{V_s}} \qquad \textbf{0-21}$$

Where T_0 = Predominant period (sec.)

$$\overline{V_s} = \frac{\sum_{i=1}^{n} V_{si} * H_i}{\sum_{i=1}^{n} H_i} \qquad \textbf{0-22}$$

V_{si}= Shear wave velocity for each layer (M/sec)
H_i= Thickness of layer (m), and
N= no of layers (excluding the rock bed).

(ii) Gravity method:

$$T = 4\sqrt{\frac{2}{g}\sum_{i=1}^{n-1}\frac{H_i}{G_i}\left(\sum_{j=1}^{i}\gamma_j H_j - \frac{1}{2}\gamma_i H_i\right)} \qquad \textbf{0-23}$$

Where

T= predominant period, sec.
n= Total number of layers, including the base layer.
γ_i= unit weight of i-th layer (t/m^3)
H_i= Thickness of the i-th layer (m)
G_i=Shear modulus of i-th layer (t/m^3)
g= Acceleration due to gravity, 9.8 m/sec^2.

(iii) Frequency Response function solutions (see section 4-3 and appendix F).

$$H_{m/n}(\omega) = \frac{A_m + B_m}{A_n + B_n} \qquad \textbf{0-24}$$

(iv) Equivalent Linear Solutions.

All the methods, except the last one, are linear methods of analysis more suited for small strain levels. The latter can be implemented using one of the readily available programs. Here a commonly applied program SHAKE is implemented [22].

In the use of SHAKE program, the Elcentro, Hachinohe and Kobe earthquake records are used for each of the 3 sites. The three records are commonly used for site effect studies, because they vary form short duration big pulse (Kobe) to high frequency rich motions (Elecentro), to long duration records (Hachenohe), thus enabling investigation under widely varying characteristics of input motions. Time histories of the input earthquakes and their Fourier spectral plots are shown in figure 4-8 and 4-9 respectively. Before analysis, the records are scaled down to magnitudes relevant to Addis Ababa area.

Geff Katon (1994) conducted a study for credible accelerations expected in Addis Ababa city and the surrounding, and has shown that the peak-ground-acceleration (PGA) of recurrence 500 years is 0.09*g*. Hence the records are scaled down to a maximum acceleration of 0.883m/Sec^2. Furthermore a maximum of 5% error in computed *G* value or maximum of 5 iterations was set as a criterion in determining strain compatible properties.

Acceleration transfer functions obtained for each site are plotted in figures 4-10 to 4-12. The results have been summarized in table 4-1. From the Fourier spectrum plots, it can be seen that:

(1) All input motions are modified by site effects;

(2) Multiple peaks are observed for each site and each input motion. The first peaks show acceptable agreements with linear analytical solutions, and with microtremor observation methods.

(3) The second peaks for the sites represent periods in the range of 0.65-1.00 sec. Because the earthquake magnitude used is relatively high (i.e., 500 years return period), the strains involved are high giving higher periods.

Figure 0-8: Acceleration time history of (a) Elcentro, (b) Hachenohe, and (c) Kobe Earthquake records.

Figure 0-9: Fourier Spectrum of Input motions

Table 0-1: Summary of Computed T0 from different methods.

S.No. (1)	Model (2)	$f(v_s)$[1] (3)	$f(\gamma,G)$[2] (4)	FESP[3] (5)	Avg. (6)	EQL[4] 1st Peak (7)	EQL[4] 2nd peak (8)	Micro-tremor (9)
1	Site I	0.2	0.184	0.18	0.188	0.27	0.65	0.17
2	Site II	0.202	0.19	0.18	0.190	0.26	0.74	0.19
3	Site III	0.27	0.25	0.24	0.253	0.25	0.97	0.22

Temporary measurements of microtremors were taken at spot designated ARA064 (Site I), ARA067 (SITE II) and ARA014 (Site III). The Fourier spectral analysis and determination of *H/V* spectral ratios for the recorded time series was carried out and results are summarized in table 4-1, above.

It is observed that the predicted results of predominant periods vary appreciably with the method of analysis, i.e. whether LINEAR or EQUIVALENT LINEAR method is used, and though less significantly with the type of earthquake used. Also resonant frequency of the sites obtained from linear analysis and microtremors analysis are comparable. Equivalent linear results for site period are higher, which is due the induced strain levels, and the resulting change of $\boldsymbol{G}$ and $\boldsymbol{\xi}$ values. As expected, a good correlation exists between results from the linear analysis method and from microtremor analysis. It can be concluded that microtremor analysis can be used to estimate the dominant resonant frequency of sites.

Figure 0-10: Strong motion Spectral ratio computed for Site I.

Figure 0-11: Strong motion Spectral ratio computed for Site II.

Figure 0-12: Strong motion Spectral ratio computed for Site III.

Figure 0-13: Plot of Fourier Spectra for Site AI A064 (near Ste I).

Figure 0-14: Plot of Fourier Spectra for Site ARA067 (near Site II).

Figure 0-15: Plot of Fourier Spectra for Site ARA014 (near Site III).

[1] Method (i)
[2] Method (ii)
[3] Computed using program FESP (Method described in section 5-3, program code available in appendix F)
[4] Results from Equivalent linear analysis of SHAKE.

Field Observation of Microtremors, Analysis and Results

General

Field observation of micro-tremors was carried out at various spots in the delineated area. Spots for microtremor observation in the study area are selected with due consideration of prevailing geologic conditions and suitability to standard requirement of the measurement procedure. The latter include:

- Minimal source effects from nearby / close sources (vehicle or pedestrian interference); and
- Distance from heavy building site and perimeter of foundation works.
- Geologic conditions include avoiding rock out crop areas.

Two groups of observational spots are identified. The first group comprises those areas where modeling of sites for theoretical response analysis is done. The second group of spots is identified for the main observation through out the delineated area of interest. Analysis of observed micro-tremor data and compiling of results is then carried out.

Observation sites

The observation spots for this thesis have been first identified from a map of the city produced by Ethiopian Mapping Agency. The intention was to obtain a random distribution throughout the delineated area. About 89 sites have been first identified. Later during field works, some points are moved to suitable locations considering prevailing conditions, and some had to be left out. The total number of spots for which microtremor measurements are taken are 81.

The list of spots used for the observation in the study area is listed in appendix A. Very few spots lie on rock outcrop or shallow soil deposit area. Figure 5-1 shows observational spots overlaying the road map of the study area.

Analysis of Data

The basic analysis of the field data requires conventional Fourier spectrum analysis. This can be done on the laptop computer accompanying the equipment for micro-tremor measurement.

An interactive program (***micrAn***) has been developed to assist the analysis method and improve concluding results. The program has been very helpful in carrying out the analysis with flexibility and accuracy. A snapshot of the user interface window, during a typical analysis, is depicted in figure 5-2. The program enables interactive selection of variable width time history segments for spectral analysis. This feature enables leaving out extreme noise areas on the time history, which cannot totally be avoided during actual field measurements.

Thus the number of segments used to characterize a particular time history at a measurement site depends on the quality of data. A time window of 20 seconds is adopted for each time history record. As much as 10 segments of time history can be separately analyzed for Fourier spectral plots using the program *micrAn*, giving S_{EW}, S_{NS} and S_{UD} components of spectral plots as obtained from

$$S = \left| FFT(y_i) \right| \qquad \textbf{0-1}$$

where *S* is the magnitude of the discrete Fourier transformed value of the sequence yi.

Figure 0-1: Microtremor Observation spots.

Figure 0-2: View of program micrAn, the user interface: showing time window, processing options, and spectral measurement features.

These components can be [optionally] stored for latter analysis, which include:

- Resultant Fourier spectral magnitude computation for the two orthogonal horizontal components, determined [in this thesis] from the relation

$$S_{RH} = \frac{S_{EW} + S_{NS}}{2} \qquad \textbf{0-2}$$

- Horizontal to vertical spectral ratio computation, as

$$HV = \frac{S_{RH}}{S_{UD}} \qquad \textbf{0-3}$$

And,

- Averaging of thus computed HV components for the various segments in the frequency domain.

Automatic computation of averaged Fourier spectral function is also done [using *Auto Mode* tool provided] which considers all selected segments of the time history in the manual analysis as a single / joined time history, and computes an averaged Fourier spectra for the new series using overlapping time windows. Once the analysis is completed for a signal history at a site, interactive measurement of spectral amplitudes (magnitudes) and frequency values is made.

In further spatial analysis of the results, the study area is characterized by variation of the following dynamic parameters:

(1) Predominant period of vibration To: This is period at which the maximum amplitude is observed in the Fourier spectrum of the analyzed time-history. It is related to the frequency of resonance as

$$T_o = \frac{1}{F_o} \qquad \textbf{0-4}$$

(2) Maximum amplitude A0: This is the maximum value of the Fourier amplitude in the spectrum plot.

These parameters can effectively be used to address the particular goals/ objectives of this thesis. The plotting of these two parameters on a base map and interpretation is carried out using Arch View / GIS®, a software popular in the analysis and interpretation of geographic information. It is ideally suited for the purpose at hand, enabling:

(1) easy incorporation of data file on to a base map

(2) Generation of Dot maps and Contour maps for desired parameters

Results and Discussions

The methods and approaches thus far developed have been applied to the data collected at 81 spots all over the central part of Addis Ababa. The Fourier spectral analysis for the sites is attached in appendix G. From the figures, it can be seen that only 67 sites show clear predominant periods and the general trend expected in Fourier spectral plots. Results from the other 14 points are not very clear in the range of interest ($0.1 < T0 < 1.0$). Peak amplitudes for these spots usually exist in the longer period range, $T > 1$ sec.

The values of the two parameters, i.e., predominant period *To* and Fourier Amplitude *A0*, obtained using program *micrAn* for all the observation spots are attached in appendix A.

Plots of the two parameters obtained from Arch View/GIS is shown, overlaying the road network map, in figures 5-3 and 5-4.

The following major observations were made:

1. Most sites showed clear and understandable peaks in spectral ratio plot of H/V component.

2. There is no large-scale variation in the magnitude of predominant period in the delineated area of interest. As such, the obtained values varied between 0.15 sec. and 0.25 sec. for most parts of the area.

3. Generally, most sites can be characterized as having lower predominant period, fairly within the range $0.1 < To < 0.2$. Southern part and few points in the northeastern part, outside of the rock outcrop areas, shows values between 0.2 and 0.3 sec.
4. Amplitude levels also show variation from site to site. Southern areas, which exhibit relatively flat topography and relatively thicker deposits, show greater value for amplification level at To.

5. Few points showed exaggerated levels of amplification (>20).

Figures 5-5 and 5-6 are contour maps produced by merging results from this work and that from the preceding work by Abera (2001) [2] for the southeastern part of the city. The maps depict the variation of site period and Fourier amplitude in the areas by contour lines of varying thickness.

Figure 0-3: Variation of Predominant period in the central part of Addis Ababa

Figure 0-4: Variation of Fourier Amplitude in the central part of Addis Ababa.

Figure 0-5: Contour map of To for both study areas

Figure 0-6: Contour map of A0 for both study areas

Conclusions and recommendation

The following conclusions and recommendations were drawn from the study.

(1) Microtremor observation showed clear and stable predominant periods for most of the sites for temporary measurements through out the central part of Addis Ababa.

(2) Results from microtremor spectral analysis and 1D equivalent linear analytical solutions at selected reference sites show similarity. There is a good correlation both in spectral amplitude and in site period.

(3) The values obtained for predominant periods show site dependent variation. Western part of the study area exhibits values between 0.10 sec. and 0.20 sec., while eastern and southern part shows values between 0.20 and 0.25 sec. on average. Values as high as 0.34 are found for southern part.

(4) The variation observed for amplitude of Fourier spectral plots is also site dependent. Southwestern part of the study area showed greater spectral amplitudes as compared to other areas.

Forthcoming works by other researchers in other parts of the city can add to the findings in this and the previous works. Finally a seismic microzonation map can be made available for the whole city. These maps can be used to prepare service map for the city, mitigative measure planning for existing structures, proper designing and implementation of future projects to come. Further works in vulnerability assessment for existing infrastructure in the city, can be easily merged with the local hazard map to attain local seismic risk definition for the city.

References

1. Asfaw, L. M., (1990) *Seismicity and Earthquake Risk in Addis Ababa Region. SINET: Ethiopia J. Sci. 13 (1)*: 15-35.

2. Abera D., (2002) *Seismic microzonation for Southeastern Addis Ababa*, *Msc. Thesis, A.A.U., Addis Ababa*.
3. Arai H., Tokimatsu K., (1988) *Evaluation of Site effects based on Microtremor H/V Spectra,)*, *ESGS*[5]*, Balkema, Roterdam*. PP 673-680.
4. Ayele G., (2001) *Seismic Microzonation of Addis Ababa*, *Msc Thesisis, A.A.U., Addis Ababa*.
5. Bonilla L. F., Lavalle D., Archulea R. J. , (1988) *Non Linear site response: Laboratory Modeling as a constraint for Modeling accelerograms*, *ESGS, © Balkema, Roterdam, Netherlands* (PP 793-780).
6. Bowels J. E., (1994) Analysis and Design of Foundations, 6th ED, © *John Willey and Sons, USA*.
7. Dorwick D. J., (1997) Earthquake resistant Design, © J*ohn Willey and Sons, Britain.*
8. EBCS-8, (1995) Ethiopian Building Code Standard, Design of Structures for Earthquake Resistance, vol. 8, © *Ministry of Works and Urban Development, Addis Ababa, Ethiopia.*
9. Gazetas G., Psarropoulis P.N., (1988) *1D & 2D Seismic Response Analysis of Alluvial Valley at a Bridge Site*, *ESGS, © Balkema, Roterdam.Netherlands* (pp 841-848).
10. Geophysical exploration for Engineering and environmental investigation, (1995) *Dept. of the army, US Army Corps of Engineers,* Manual no. EM 1110-1-1802
11. Guin P.,(1978) Earthquake History of Ethiopia and the horn of Africa.
12. Haile M., (1996) *Critical Assessment of site effect parameters for strong ground motion prediction*, Doctoral Thesis, Tokyo, Japan.
13. Haile M., (1988) *Study of Site Effects at Axum obelisk Site by using Microtremors*, ESGS © Balkema, Rotterdam. Netherlands PP 665-671.

[5] ESGS: Effects of Surface Geology on Seismic Motion

14. Haile M., Seo K., Kurite K., Kyuke H., Yamanaka, Yamazaki K., Nakamaru A., *Study of Site effect in Kobe area using microtremors*, (1998) Proc. Of 2nd International symposium on ESGS © Yokohama, Japan.

15. Huang H. C., S. T. Wu, (1988) *Site effect Evaluation in the Yun-Chia-Nan area, Taiwan using H/V ratio,* ESGS © Balkema, Rotterdam. Netherlands (PP 681-687).

16. Kazuoh S., (1988) *Application of Microtremors as Substitute of Seismic Motion - reviewing the recent Microtremor joint research in Different Sites*, ESGS © Balkema, Rotterdam. Netherlands (PP 577 – 586).

17. Kobayashi H., (1991) *Application of Microtremors measurement for urban planning*, Proc. Of 5th Int. Conf. On Seismic Zonation, © Oues Editions Nice, France.

18. Kramer L. Steven, (1996) Geotechnical Earthquake Engineering, © Prentice-Hall, Inc., USA.

19. Mauro D., (1995) *Vulnerability assessment, topics of Discussion*, Proc. Of 5th International Conf. On Seismic Microzonation, © Ouest Editions, Nice, France.

20. Nozomu Yoshida, Hiroyoshi kiku, Iwauo Suetomi, (1988) *Earthquake Response Analysis under very severe earthquake*, ESGS © Balkema, Rotterdam. Netherlands (PP 757-764).

21. Oshaki Y., (1982) *Dynamic characteristics and 1 Dimensional Linear amplification theories of soil deposits*, Dept. of Architecture, Faculty of Engineering, University of Tokyo, Research Report 82-01.

22. Schinabel P.B., Lysner J., Seed H. B., (1972) *SHAKE - Computer Program for Earthquake response analysis of horizontally Layered Sites, Report No. EERC 72-12*, College of Engineering, University of California, Berkeley, California.

23. Signal processing tool box, Users guide (1988-1999), © *The Math Works Inc.*

24. Tim Law k., Qiang Song, (1988) *Effects of Alluvial Valley on Seismic ground motion*, ESGS © Balkema, Rotterdam. Netherlands pp 849-857

25. Toshinawa T., Nashida H. , Midorikawa S. ,Aba S. , (1988) *Comparison of spectral Characteristics of Strong Ground Motion and Microtremors at dense strong ground motion sites in Yokohama*, ESGS, © Balkema, Rotterdam. pp 399-406.

26. Tsehayu K., Hailemariam T., (1990) *Engineering geological mapping of Addis Ababa*, Ethiopian institute of geological survey, Addis Ababa. (Unpublished)

27. Woreda Map of Addis Ababa, Region 14 Bureau of Works and Urban development, (unpublished).

Appendices

List of Microtremor observation spots

The List of spots identified for microtremor observation, their Cartesian location in Easting (meters) and Northing (meters) and obtained results of predominant period and resonant frequency is listed below.

Table_ 0-1: List of Microtremor observation spots, Location and results of analysis

S.No.	CODE	Easting, m	Northing, m	Period, sec.	Amp., A0	SITE NAME
1	'ARA001'	474901	995945			'BIBLESOCIETY'
1	'ARA001'	474485	995965			'BIBLESOCIETY'
2	'ARA002'	474357	996241	0.24	15.4	'LRNRSCRNR'
3	'ARA003'	474421	996385	-		'BERHANEWONGEL_CHRCH'
4	'ARA004'	474541	996189	-		'CASA_INCHIS'
5	'ARA005'	474785	996133	0.20	0.8	'CASA_INCHIS2'
6	'ARA006'	474505	996637	0.13	2.3	'GOJO_RSTRNT'
7	'ARA007'	473880	996369			'PLC_STN'
8	'ARA008'	474128	996841			'ADWAPARK'
9	'ARA009'	473532	997169			'HILTON_SIDE'
10	'ARA010'	473272	997049	0.30	3.9	'SHERATON_NRTO'
11	'ARA011'	473280	996801	0.24	53.7	'SHERATON2'
12	'ARA012'	472868	996193	0.21	4.1	'MOSQUE'
13	'ARA013'	472188	996253	0.24	10.1	'KEDJA'
14	'ARA014'	471970	996105	0.23	24	'SHEBELLE'
15	'ARA015'	472404	996068	0.34	8.9	'LERNERS_CRNR'
16	'ARA016'	472396	996411	0.31	8	'COMMERCE'
17	'ARA017'	472454	996472	0.16	7	'TROPICAL_HTL'
18	'ARA018'	472318	996634	0.25	43.1	'CULTURE_MINSTR'
19	'ARA019'	472183	996597	0.18	22.4	'WOMEZEKIR'
20	'ARA020'	472571	997115	0.21	44.7	'TYRE_ECON'
21	'ARA021'	472770	997166	-		'IMIGRATION'
22	'ARA022'	472837	997402	-		'BLION_SCHL'
23	'ARA023'	473137	997462	0.16	1.7	'LICEFRANCOPHONE_REAR'
24	'ARA024'	473148	997690	0.24	3.7	'ROADSIDE'
25	'ARA025'	472725	997729	0.27	5.6	'ETHIOVISSION_CLNC'
26	'ARA026'	472231	997790	0.28	1.9	'MEGATHEATER'
27	'ARA027'	473324	996008	0.14	25.3	'EXTREME_HTL'
28	'ARA028'	473163	996167	0.17	8.8	'STADIUM1'
29	'ARA029'	472916	996378	0.18	43.2	'STADIUM2'
30	'ARA030'	472654	996324	0.18	25.6	'DPPC'
31	'ARA031'	472599	996035	0.22	5	'RAS_HTL'
32	'ARA032'	472695	996119	0.16	22.2	'WORKS_MINSTR'
33	'ARA033'	473421	996214	0.14	36.8	'SAINT_MARY_CHRCH'
34	'ARA034'	473623	996078	0.20	13	'GHION1'
35	'ARA035'	472801	996838	0.31	6.9	'GHION2'
36	'ARA036'	472502	996696	0.12	11.4	'PO_PARKNG'
37	'ARA037'	472262	997166	0.21	2.3	'BOARD_VOTE'
38	'ARA038'	472366	997352	0.14	22.9	'YEHULU_CLNC'
39	'ARA039'	471735	997677			'GOLAMICAEL_CHRCH'
40	'ARA040'	471805	998013	0.24	15.4	'T/HAIMANOT_CHRCH'

S.No.	CODE	Easting, m	Northing, m	Period, sec.	Amp., A0	SITE NAME
41	'ARA041'	471948	998230	-		'SOMALI_TERA'
42	'ARA042'	472242	998078	-		'ALIANCE'
43	'ARA043'	472901	998402	0.20	0.8	'CATHEDRAL_CHRCH'
44	'ARA044'	472589	998817	0.13	2.3	'AMPERE'
45	'ARA045'	472748	999192			'SANJORGE_CHRCH'
46	'ARA046'	472672	999116			'AARESTURANT'
47	'ARA047'	472287	999238			'3POLICE_STN'
48	'ARA049'	471847	999194	0.30	3.9	'WSSA_REAR'
49	'ARA050'	471729	998950	0.24	53.7	'ST.JORGE_CHRCH'
50	9'ARA051'	471891	998705	0.21	4.1	'ABAKORAN'
51	'ARA052'	472102	998640	0.24	10.1	'TALIAN_SEFER'
52	'ARA053'	472378	998976	0.23	24	'TALIANSEFER2'
53	'ARA054'	472774	999626	0.34	8.9	'UNKNOWN'
54	'ARA055'	473192	999452	0.31	8	'AFINCHO_BER'
55	'ARA056'	473463	999345	0.16	7	'40_DEREJA'
56	'ARA057'	473281	999098	0.25	43.1	'YEKATIT12_HSPTL'
57	'ARA058'	473765	998497	0.18	22.4	'NAZARETH_SCHL'
58	'ARA059'	473688	997824	0.21	44.7	'CPA_REAR'
59	'ARA060'	473708	998072	-		'ROADSIDE'
60	'ARA061'	474183	998110	-		'ROADSIDE'
61	'ARA062'	474044	998406	0.16	1.7	'SELASIE_CHRCH'
62	'ARA063'	473565	998916	0.24	3.7	'SCIENCE_FACULTY'
63	'ARA064'	473674	999113	0.27	5.6	'MUSEUM_REAR'
64	'ARA065'	473750	999314	0.28	1.9	'SGS_5KILLO'
65	'ARA066'	474044	998627	0.14	25.3	'LION_ZOO'
66	'ARA067'	474296	999121	0.17	8.8	'MNILIK_SCHL'
67	'ARA069'	474497	998739	0.18	43.2	'UNKNOWN'
68	'ARA071'	474544	998910	0.18	25.6	'UNKNOWN'
69	'ARA072'	474827	998804	0.22	5	'BASHACHILOT'
70	'ARA073'	474202	998871	0.16	22.2	'FERESEGNA'
71	'ARA074'	475062	998611	0.14	36.8	'MNILIK_SCHL_REAR'
72	'ARA075'	475263	998290	0.20	13	'KEBENA_1'
73	'ARA076'	474827	998619	0.31	6.9	'KEBENA2'
74	'ARA078'	474553	998326	0.12	11.4	'BRITISCH_SCHL'
75	'ARA079'	475405	998700	0.21	2.3	'ANGLICAN_CHRCH'
76	'ARA081'	475610	997976	0.14	22.9	'ROYAL_ACADEMY'
77	'ARA082'	475209	998082			'ROADSIDE'
78	'ARA083'	475308	997819	0.24	15.4	'BELAIR_HOTEL'
79	'ARA084'	475381	997443	-		'MONALIZA_HTL'
80	'ARA086'	475189	997499	-		'AWARE2'
81	'ARA087'	474425	997970	0.20	0.8	'AWARE3'
82	'ARA088'	474799	998061	0.13	2.3	'BALEWOLD_CHRCH'
83	'ARA089'	471923	996421			'AWARE/KEBENA'
84	'ARA090'	471971	996781			'DAFRIQUE'
85	'ARA091'	472075	997547			'BLION_NRTO'
86	'ARA093'	471633	998525	0.30	3.9	'GARAD_BLDG_REAR'
87	'ARA094'	472510	998365	0.24	53.7	'GOJAM_BERENDA'
88	'ARA095'	472856	998049	0.21	4.1	'ARADA_BLDG'
89	'ARA096'	474901	995945	0.24	10.1	'TAITU_HTL'

Borehole logs, and soil data for the three selected sites

Three model sites are used for analytic modeling. Site-I represents a bore hole at Technology Faculty, AAU, 5 killo. Site-II represents a bore hole located in Science Faculty of AAU, 4 Killo. And Site-III represents that near Wabe Shebele Hotel, Mexico area.

At some depths recorded N values show exaggerated figures for the layer description associated with it. Because the description of soil layers and strata is based on visual classification during the logging, the observed N values are used as a reliable data for computing dynamic response behavior.

Table_ 0-1: Borehole log and description for Site-I.

Depth range, m	Description
0.00-0.20	Top soil
0.20-1.50	Backfilled soil
1.50-4.20	Red silty clay soil
4.20-5.50	Reddish gray clayey silt
5.50-6.20	Silt mixed with clay at intervals
6.20-8.45	Silt soil mixed with highly weathered basaltic gravels at intervals
8.45-10.00	Highly weathered basaltic boulders

Table_ 0-2: Blow count records for Site-I.

Depth	N values	Remarks
1	18	
2	33	
3	26	
4	15	
5	13	
6	13	
7	46	
8	39	

Table_ 0-3: Borehole log and description for Site-II.

Depth range	Description
0.00-0.30	Top soil
0.30-1.00	Dark gray clay
1.00-1.50	Basaltic boulders
1.50-2.00	Dark gray clay
2.00-3.00	Yellowish gray clay
3.00-4.00	Highly decomposed soft rock
4.00-7.30	Highly decomposed soft rock with clayey silt
7.30-9.70	Vesicular soft rock mixed with silt
9.70-10.5	Vesicular basaltic gravel
10.5-11.6	Vesicular basaltic rock with gravel at intervals

Table_ 0-4: Blow count records for Site-II.

Depth, m	N values	Remarks
3.3	16	
4.3	14	
5.3	15	
6.3	20	
8.0	60	

Table_ 0-5: Borehole log and description for Site-III.

Depth range, m	**Description**
0.00-0.40	Top soil
0.40-0.80	Dark brown clay
0.80-2.20	Weathered trachytic rock
2.20-6.50	Compacted red clay
6.50-7.40	Weathered basalt rock
7.40-9.10	Weathered porous basalt rock
9.10-13.00	Highly weathered basalt rock
13.00-16.50	Sandy silt
16.50-20.00	Weathered basalt gravels with boulders at intervals
20.00-24.00	Weathered porous basalt rock

Table_ 0-6: Blow count records for Site-III.

Depth, m	**N values**	**Remarks**
3.3	11	
4.2	19	
5.1	26	
5.7	32	
6.1	16	
6.9	34	
7.7	12	
8.3	12	

Laboratory test results extracted, as used for computation of G/G_{max} and ξ vs. γ relations in chapter 5 are listed below.

Table_ 0-7: Laboratory test results for soil samples from bore-holes.

Bore hole ID or site	Depth Range	*PI* (%)	γ (t/m$_3$)	γ(t/m^3) generated[6]
Site-II: Science Faculty of AAU	2-7 7-9 9-12	52 20 0	1.7 1.8 1.85	1.709 1.833 1.833
Site-III: Mexico area	1-8 8-25	55 0	1.70 -	1.60 1.95

Note: Laboratory test results for Site-I were unavailable. Values approximately equal to that in Site-II are used as one is located in the nearby vicinity of the other.

Results for G/G_{max} and ξ are obtained for the input parameters shown in table 5-4 and have been plotted in figure 5-2.

Table_ 0-8: Values of PI, γ and σ_m as used in determining γ vs. G/Gmax and γ vs. ξ relations.

Site Name	Depth	PI(%)	γ(t/m3)	σ_m(KN/m^2)	G_{max}(t/m^2)
Tech. Faculty (Site-I)	0.0-2.5	52	1.6	19.62	5620
	2.5-4.5	52	1.6	54.94	12350
	4.5-10.0	0	1.90	123.238	18790
Science Faculty (Site-II)	0.0-7.15	52	1.70	59.62	8120
	7.15-9.25	20	1.80	137.78	18870
	9.25-12.00	0	1.85	275	27362
Mexico Area (Site-III)	0.0-5.90	55	1.70	49.197	8240
	5.9-7.3	55	1.70	110.06	14580
	7.3-20.0	0	1.85	145.589	20990
	20.0-25.00	0	1.95	314.187	36360

Note: Confining pressure, σ_m, is calculated at the middle of each layer.

Soil Dynamic properties

Corrected N_{60} values. The N valves recorded during investigation are a function of soil type, confining pressure and soil density, and also influenced by test equipment and procedures. It has become common to normalize the N value to an over-burden pressure of 1.0 t/ft^2 (100Kpa) and to correct it to an energy ratio of 60% (average ratio of the actual energy delivered by the hammer to theoretical free fall energy). The relation can be defined as [18]:

$$N_{60}=N_r C_N \frac{E_m}{E_{ff}}$$

Where,

N_r = Recorded below count,
E_m = Actual hammer energy,
E_{ff} = Theoretical free fall energy, and
C_N = An over burden correction factor given by

$$C_N=\sqrt{\frac{95.76}{\sigma_{vo}}}$$

And σ_{vo} (KPa) calculated at middle of each layer.

There is no information or background study on the values of (percent of) E_{ff} to be used as energy transfer ratio (ETR in E_m= ETR*E_{ff}) to obtain the actual hammer energy. Ranges of measured values by researches abroad include 0.35-0.80. To study the variability and degree of dependence of the object function, i.e.,

[6] Unit weight values generated during soil simplification process.

predominant period ***To***, to this variable ETR (and also to a soil simplification parameter COEF discussed in appendix C), parametric study is carried out (see appendix E).

Shear wave velocity, Vs:- This is a critical parameter influencing the dynamic response behaviors of the soil layer it represents. It is most appropriately obtained from field tests by geophysical methods. In the absence of this, as in the data we have here, empirical relations are used. A relation proposed by Ohta and Goto (1976) is

$$Vs\ (m/sec) = 68.79\ N^{0.171}\ H^{0.199}\ E\ F$$

Where

E (Epoch) = 1.000 for alluvium
= 1.3030 for diluvium

F (Facies) = 1.000 for clay
= 1.086 for fine sand
= 1.066 for medium sand
= 1.135 for coarse and
= 1.153 for sandy gravel
= 1.448 gravels

The value for Facies (F) is assigned basically using the soil type composition. Hence

F= 1.00 for type 'CC' or clay and silt soils,
=1.086 for type 'SC', for sandy clays or sandy silts, and
=1.153 for type 'SS', for sands and gravels

The results obtained thus are used in determining shear modulus G_o from a suitable relation.

Shear Modulus, G_0: This parameter can be computed from one of the various methods outlined in section 4-4. Table C-1 below shows G_o values computed for Site-I using the methods in section 4-4. The values of ***Go*** obtained form these relations are not very similar. In fact, there is a significant scatter in obtained values from various researchers. The difficulty arises mainly because correlation is between a small strain parameter ***Go*** with large strain parameter ***N***. Hence the values shall be treated with caution.

Table_ 0-1: Computed values for Go using the various methods for site I

Depth, m	(, t/m3	(, (t/m2)	N	Shear Modulus, Go, computed by various methods[7]						
				(i)	(ii)	(iii)	H	F	Vs	(iv)
0.0-2.5	1.6	2	23	14742	13391	5760	1.25	1	160	4185
2.5-4.5	1.6	5.6	33	19679	17116	11432	3.5	1.0	211	7276
4.5-10	1.9	12.425	27	16760	14933	16585	9.75	1.4	347	23304

The same trend is observed for other sites as well. And in conclusion, it can be seen that methods (i) and (ii) show exaggerated values at / near the surface and heavily biased trend with that expected for increasing depth. Method (iii) and (v) gave preferable results. An approximation to the predominant period T_0 of a given soil profile may be obtained using the 'Gravity Method', which is obtained from equation 4-23.

[7] The methods of obtaining Go values are described in chapter 4, equations 4-12 to 4-15. They are named methods (i) to (iV) respectively.

Using G values from methods (iii) and (iv), T_0 in equation *4-23*, evaluates to 0.139 sec. and 0.135 sec. respectively, and are not very much different. Method (iii) has been used for computing Go values in further works.

Soil profile simplification

Soil simplification procedure is used to change a given (natural) soil profile logging so as to be suitable for dynamic analysis. This is necessary because usually soil profile loggings are complicated beyond practical significance. The soil type in each layer in the original borehole record and N-values of the standard penetration test approximately at equal intervals are required.

Influence of variables Energy Transfer Ratio, (ETR) and soil simplification coefficient (COEF) on Computed period (To)

As discussed in relevant sections of the body of this thesis, there is little or no information on the values of Energy Transfer function (ETR) to be used in adopting the recorded N values to practical application. An introduction of soil simplification procedure in the analysis for dynamic response behavior of soil deposits, with a wide range of values recommended for the governing coefficient, takes off a certain level of confidence on the values obtained for the objective function, i.e., ***To***.

A spatial analysis of variability of predominant period with these two parameters is carried out. Sensitivity indicators are also computed with gradient of the function for ***To***. Graphical representation of results is attached for one of the sites.

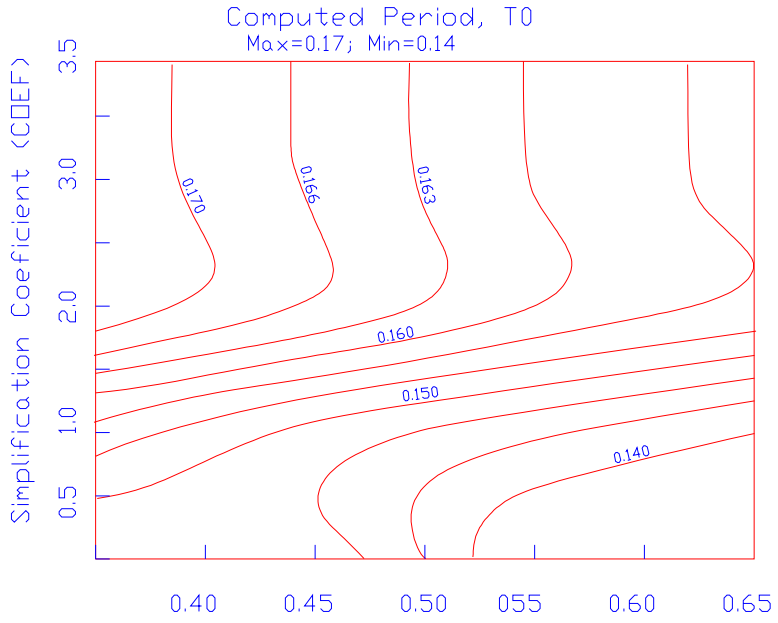

Figure_ 0-1: Graph of computed period, T0, as a function of soil simplification coefficient (COEF) and Energy transfer Function (ETR) for soil profile at site-I.

The following observation was made from the trends of variation in the graphs.

1. The computed period of deposits is influenced by both parameters (i.e, COEF and ETR).
2. Maximum period is obtained for low ETR values and Higher COEF values.
3. The effect of reduced ETR is to reduce corrected N values resulting in less stiff material and hence increased ***To***. This is well explained in the graphs.
4. Computed period is more sensitive to COEF than to ETR.

5. Especially near practical recommendations, computed period is less sensitive to ETR. It can be concluded that using values for parameter COEF between 1.0 and 1.5, more or less similar values are expected, even if values of ETR are not very accurate.

The modeling of soil profiles is therefore carried out with the following set of parameters.

Table_ 0-1: Recommended values of Energy Transfer Ratio (ETR) and soil simplification Coefficient (COEF) for each of site as obtained from parametric study.

Site name (Description)	Recommended values	
	COEF	ETR
Technology Faculty (BH #2)	1.50	0.4
Science Faculty (BH #2)	1.00	0.4
Mexico area	1.00	0.45[8]

[8] This is to account for use of 70 kg hammer used in the SPT.

$N_1E_1=N_2E_2$

=> $N_{60}=N_{70} * E_{70}/E_{60} =N_{70} * 70/60 = 1.10\ N_{70}$;

and $N_c = N_r C_N \frac{Em}{0.6E_{ff}}$, where $N_r=1.10\ N_{70}$ and $E_m= 0.40$ gives

$$N_c = N_{70} C_N \frac{0.45E_{ff}}{0.6E_{ff}}$$

Frequency response analysis program

The formulation of linear solution to dynamic analysis of layered soil systems has been outlined and used in chapter 5 and is detailed in [21]. Here a source code in MATLAB as used in this thesis to obtain solutions to modeled sites is listed.

```
function fesp()

%sample Data
gama=[1.5 1.67 1.85 1.95];    %n= no of layers including bed rock
th  =[3.8 3.2 3.9];           % N= n-1
G0  =[1200 2890 5690 49670];          %N= n
damp =[.02 .02 .02 .02];              %N= n-1
% Initialization
lobj=1; lref= length(gama);Nfreq= 1000; delf= .02;
Gcomp=G0.*complex(1,damp.*2);
for i= 1: length(gama)
  P(i)= sqrt(gama(i)/9.81/Gcomp(i));
end
for i= 1: length(gama)-1
  R(i)= Gcomp(i)*P(i)/Gcomp(i+1)/P(i+1);
end
A(1)= 1; B(1)=1;w=0;

for k= 2: Nfreq;
  w= w + 6.283185*delf;
  for i= 1: length(gama)-1;
    exp_a= exp(complex(0,1)*P(i)*w*th(i));
    exp_b= exp(-1*complex(0,1)*P(i)*w*th(i));
    A(i+1)=((1+R(i))*A(i)*exp_a + (1-R(i))*B(i)*exp_b)*0.5;
    B(i+1)=((1-R(i))*A(i)*exp_a + (1+R(i))*B(i)*exp_b)*0.5;
  end
  ea=A(lobj)+ B(lobj);
  eb=A(lref) + B(lref);
  H(k)= abs(ea/eb);
  faxis(k)= k*delf;
end
plot(faxis, H)
```

Fourier Spectral Plots

The Fourier spectral analysis carried out for the 81 observational sites was carried out using the program ***micrAn***. During the analysis the result can be saved in a file for latter processing, like plotting as attached below.

Figure 0-1: Plot of Fourier amplitude vs. Frequency (Site: 002-016)

Figure 0-2: Plot of Fourier amplitude vs. Frequency (Site: 017-028)

Declarations

I the undersigned certify that that this is my work, it has not been previously submitted to any university, and that all sources of materials have been duly acknowledged.

Name: **Araya Mengistu**

Signature: _____

Date: **July 11th, 2003**

Date of Submission: July 11th, 2003.